National Research
FLAGSHIPS
Wealth from Oceans

CSIRO

Remote sensing for light attenuation mapping in the North Marine Region

Thomas Schroeder, Arnold G. Dekker and Chris Rathbone
May 2009

To: The Department of the Environment, Water, Heritage and the Arts

www.csiro.au

Australian Government
Department of the Environment, Water, Heritage and the Arts

Remote Sensing for light attenuation mapping in the North Marine Region
A report to the Department of the Environment, Water, Heritage and the Arts

ISBN 978-0-643-09736-0
Published by CSIRO Land and Water
May 2009

This publication should be cited as:

Schroeder Th., Dekker A.G., and Rathbone C., (2009), Remote sensing for light attenuation mapping in the North Marine Region, Report to the Department of the Environment, Water, Heritage and the Arts, CSIRO Land and Water, 25 pp., ISBN 978-0-643-09736-0.

Contents

List of Figures

List of Tables

List of symbols and acronyms

Symbol	Parameter	Unit
E_{d}	Downwelling irradiance	$\mathrm{W\,m^{-2}\,\mu m^{-1}}$
K_{d}	Diffuse light attenuation coefficient	$\mathrm{m^{-1}}$
$\overline{K_{\mathrm{d}}}$	Mean diffuse light attenuation coefficient	$\mathrm{m^{-1}}$
K_{w}	Diffuse light attenuation coefficient of pure water	$\mathrm{m^{-1}}$
L_w	Water-leaving radiance	$\mathrm{W\,m^{-2}\,sr^{-1}\mu m^{-1}}$
z	Depth	m
λ	Wavelength	$\mathrm{nm},\ \mu\mathrm{m}$

Acronym	Meaning
CSIRO	Commonwealth Scientific and Industrial Research Organisation
CLW	CSIRO Land & Water
DEWHA	Department of the Environment, Water, Heritage and the Arts
EOS	Earth Observing System
EPBC	Environment Protection and Biodiversity Conservation
FOV	Field of view
HDF	Hierarchical Data Format
MODIS	Moderate Resolution Imaging Spectrometer
NASA	National Aeronautic and Space Administration
NOAA	National Oceanic and Atmospheric Administration
NMR	North Marine Region
NRSMPA	National Representative System of Marine Protected Areas
PDF	Printable Data Format

Chapter 1

Introduction

1.1 Project objectives

This project develops information from remotely sensed light attenuation and bathymetry data to estimate where, on average, light penetrates sufficiently into the water column to allow photosynthesis. This physical data set then can be used as a surrogate to predict biodiversity within the North Marine Region (NMR), as part of the Australian Government marine bioregional planning process (figure 1.1). The North Marine Region covers all Commonwealth waters from the western side of Cape York to the Northern Territory - Western Australian border. It spans an approximate area of $715\,000\,\mathrm{km}^2$ covering the Timor Sea, Joseph Bonaparte Gulf, the Arafura Sea and the Gulf of Carpentaria (*DEWHA*, 2007).

Further, this project aims to address part of Goal 2 of the *Goals and Principles* determined from the guidelines set out for the National Representative System of Marine Protected Areas (NRSMPA). Goal 2 states *"The Marine Protected Area network should cover all depth ranges occurring in the Region or other gradients in light penetration in waters over the continental shelf"*. Ocean depth is one of the main factors determining distribution of biological communities. Ocean depth reflects certain basic physical variables - such as light penetration and pressure - that determine what types of animals and plants are found in particular locations. The North Marine Region includes an extensive expanse of relatively shallow water over the continental shelf. In these shallow systems it is turbidity, rather than water depth, that is the primary determinant of light penetration. It is likely that pelagic productivity and biological diversity will be determined mainly by light penetration rather than ocean depth in the North Marine Region. Results from this report may assist in developing a better understanding of this marine environment, and consequently in the marine bioregional planning process for the North Marine Region.

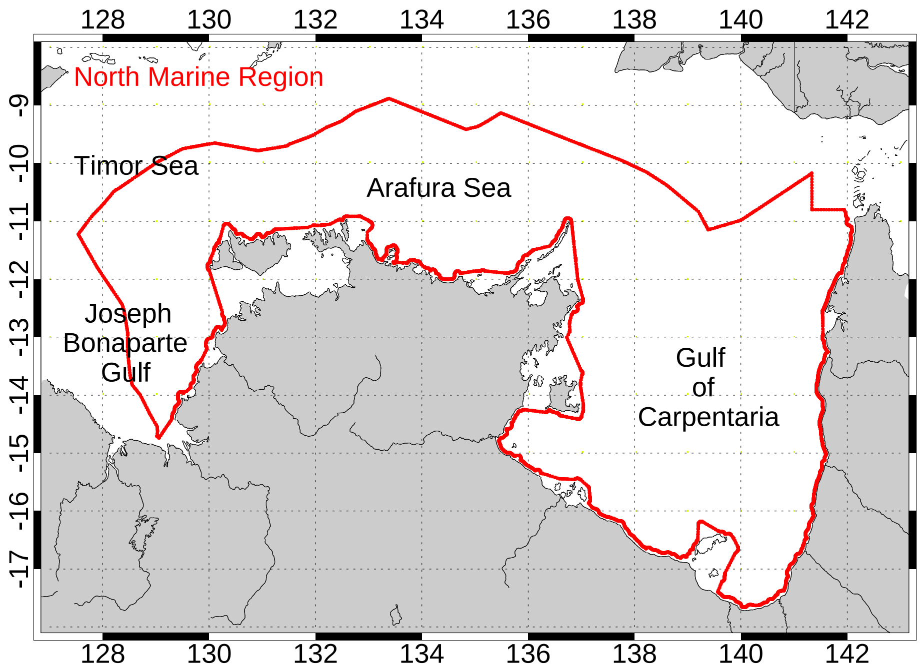

Figure 1.1: Study area with the boundary of the North Marine Region.

1.2 Background and significance

Marine bioregional planning is a process being undertaken by the Department of Environment, Water, Heritage and the Arts (DEWHA) that is designed to facilitate higher levels of protection to marine environments, conserve biodiversity and deliver greater planning certainty to industry. The Minister for the Environment, Water, Heritage and the Arts must consult a Marine Bioregional Plan when making decisions under *Environment Protection and Biodiversity Conservation (EPBC) Act 1999* for which a plan has relevance. Marine bioregional planning is a process through which the Australian Government identifies areas within Commonwealth waters for inclusion in the National Representative System of Marine Protected Areas. The development of marine bioregional plans for each of Australia's five large-scale Marine Regions provide an opportunity to make substantial progress towards this goal.

The planning process requires up-to-date scientific information on the marine environment, to identify threats and areas that may need protection. As the management of marine protected areas may require conditions to be imposed on the nature and the type and extent of human activity that may occur within them, the identification of areas suitable for inclusion in the National Representative System of Marine Protected Areas needs to be based upon clear goals and principles. This approach seeks to draw on the best available science and data. While recognising from the outset that the information base maybe poor for some areas because of their remoteness, remote sensing may provide an effective tool for providing high temporal and spatial information for otherwise data-sparse regions.

Results from this project may improve understanding of biological communities in the North Marine Region and assist in identifying potential marine protected areas as part of the Australian Government's marine bioregional planning process.

1.3 Project outline

Within this project, information on light attenuation is derived from remote sensing data acquired by the MODerate-resolution Imaging Spectrometer (MODIS) onboard the NASA Earth Observation System (EOS) Aqua spacecraft. The data in this project spans the period between 2002 and 2008. Figure 1.2 illustrates the different processing steps in the project. CSIRO processed and analyzed six aggregated inter-annual cycles of diffuse light attenuation coefficients for northern Australia's wet (November to March 2002-2007) and dry (April to October 2003-2008) seasons. The spatial resolution of the data has been set to a 4 km grid size for the assessment of light availability. The satellite data was obtained directly from NASA and re-processed to meet the spatial and temporal requirements of this project. Regions were mapped where on average, sufficient light penetrates to allow photosynthesis, for the determination of potentially high and low areas of productivity in the North Marine Region.
The aims of this project are in detail:

- To acquire and analyse satellite remote sensing data to determine light availability by means of diffuse light attenuation coefficients (K_{d}) in the water column for primary productivity assessment in the North Marine Region. The assessment of primary productivity is not part of this project.

- To determine temporal variation in light availability by means of diffuse light attenuation coefficients across the North Marine Region on an inter-annual scale for aggregated wet and dry seasons.

- To identify any remote sensing anomalies in the North Marine Region during the analysis of the data that may warrant further investigation.

- To acquire and analyse satellite remote sensing data to determine light availability at the seabed for primary productivity and benthic biodiversity (as a proxy) assessment in the North Marine Region. Note: The assessment of primary and benthic biodiversity is not part of this project.

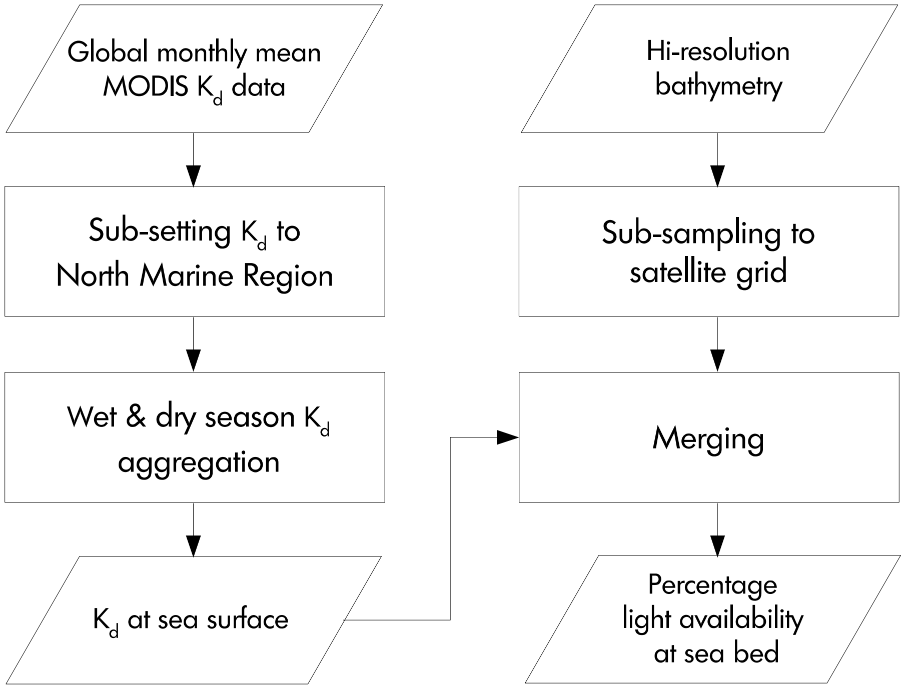

Figure 1.2: Processing flow chart of this study.

Chapter 2

Detailed sensor, data processing and algorithm description

2.1 The MODIS Aqua radiometer

High sensitivity and a large dynamic range enables the MODIS radiometer, operational since May 2002 on board of NASA's EOS Aqua polar-orbiting spacecraft, to accurately monitor the Earth's atmosphere and surface. With the spacecraft orbiting sun-synchronous at an altitude of 705 km, the imaging radiometer MODIS measures the reflected solar radiation in 36 spectral bands ranging in wavelength from $0.41\,\mu\mathrm{m}$ to $14.5\,\mu\mathrm{m}$, with a spatial resolution of 250 m (2 bands), 500 m (5 bands) and 1.000 m (29 bands) at nadir. The instrument views the Earth's surface over a $\pm 55°$ field-of-view (FOV) range relative to the instrument nadir in across-track direction using a two-sided scan mirror that rotates at $20.3\,\mathrm{r\,min^{-1}}$ (*Xiong and Barnes*, 2006). Each scan covers an across track swath of 2.330 km and Aqua's celestial orbit allows MODIS to cover the Earth's surface completely in $1 - 2$ days (figure 2.1). High spectral, spatial and temporal resolution makes the MODIS instruments ideal for the monitoring of both aquatic and terrestrial environments, including remote areas such as the North Marine Region.

2.2 NASA's diffuse light attenuation algorithm

The light attenuation in the water column at depth z, as a function of the spectral downwelling irradiance $E_\mathrm{d}(\lambda, z)$ is described by the Beer-Lambert Law:

$$E_\mathrm{d}(\lambda, z) \;=\; E_\mathrm{d}(\lambda, 0^-)\, e^{-K_\mathrm{d}(\lambda,z)\, z} \tag{2.1}$$

where $K_\mathrm{d}(\lambda, z)$ is the diffuse light attenuation coefficient, averaged over the depth range

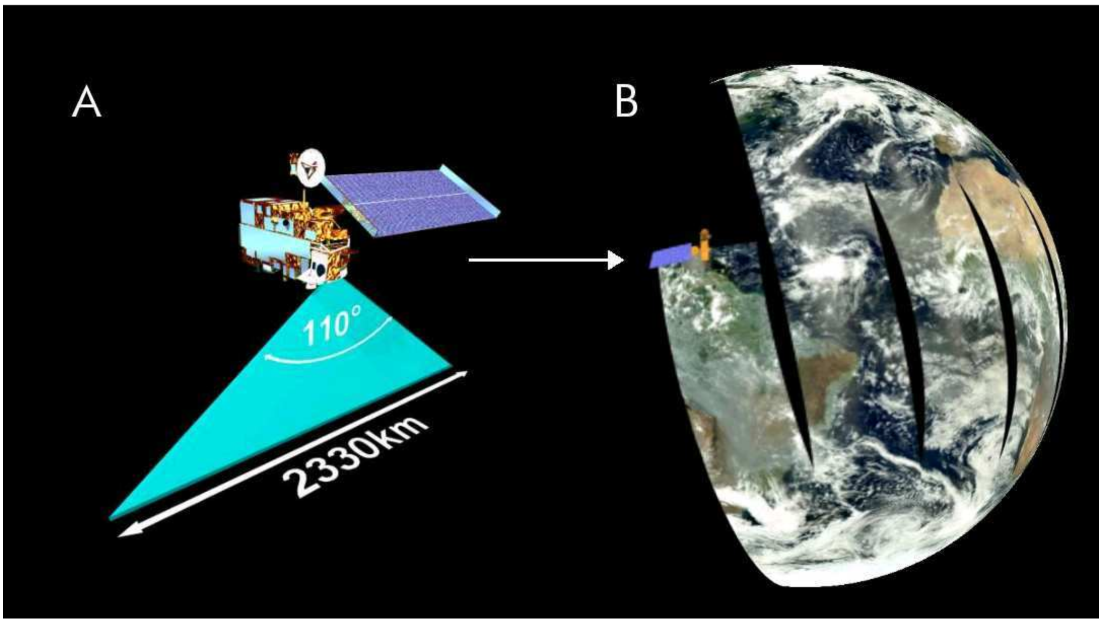

Figure 2.1: Swath illustration of MODIS (A) and polar orbiting principle of the Aqua satellite with the MODIS instrument scanning the upward reflected light of the Earth (B). Image credit: NASA and NOAA.

from just beneath the sea surface ($z = 0^-$) to the depth z in meters (*J. E. O'Reilly and 24 Co-authors* , 2000). Within this project the diffuse light attenuation coefficient is calculated from an empirical algorithm at a wavelength of $\lambda = 490\mathrm{nm}$ based on the relationship between $K_\mathrm{d}(490)$ and the water-leaving radiance (L_w) in the blue-green region of the solar spectrum (*Austin and Petzold*, 1981), (*J. E. O'Reilly and 24 Co-authors* , 2000). The light attenuation coefficient is a measure of how the visible light in the blue-green region of the solar spectrum penetrates within the water column, which is directly related to the amount of dissolved and particulate material and is an indication of the turbidity of the water column. The diffuse attenuation coefficient is calculated according to equation 2.2 from the ratio of the water-leaving radiance at two wavelengths $\lambda 1 = 488$ nm (blue) and $\lambda 2 = 551$ nm (green) as measured by MODIS with the coefficients $\mathrm{A} = 0.15645$ and $\mathrm{B} = -1.5401$. K_w is the light attenuation of pure water as published from measurements by *Pope and Fry* (1997).

$$K_\mathrm{d}(490) \; = \; K_\mathrm{w}(490) + \mathrm{A} \; \left[\frac{L_\mathrm{w}(\lambda 1)}{L_\mathrm{w}(\lambda 2)} \right]^\mathrm{B} \tag{2.2}$$

Within this project the percentage light availability at sea bed is calculated from equation 2.1 by incorporating depth information from bathymetry data (section 2.5).

2.3 Algorithm assumptions and limitations

The empirical light attenuation algorithm (equation 2.2) makes the assumption that the composition of the water column is vertically homogenous or well-mixed. These conditions are observed mostly during winter months (dry season) as reported by *Church and Forbes* (1983) when convective overturn, due to heat loss from the surface, ensures well-mixed conditions. However, in the wet season (summer), differences between surface and bottom temperatures may be as large as $5°\mathrm{C}$ leading to stratification. Close to the coast well-mixed conditions prevail throughout the year with the exception of short periods after heavy rainfall events and associated runoff.

Lee et al. (2005) evaluated empirical and semi-analytical algorithms for estimating light attenuation coefficients by comparing estimated K_d values with those calculated from in-situ profiles of the downwelling irradiance E_d (equation 2.1). The authors found that the empirical algorithm (equation 2.2) systematically underestimates K_d at values greater than $0.2\,\mathrm{m}^{-1}$. For the aggregated dry and wet seasons of the North Marine Region we observe maximum K_d values of $0.57\,\mathrm{m}^{-1}$ (dry season) and $0.55\,\mathrm{m}^{-1}$ (wet season), resulting in an underestimation of K_d in 5.8% and 5.92% respectively, of the total region - mainly in coastal waters.

2.4 Quality control, data reduction and aggregation

The global monthly averaged K_d data (Level-3 quality) obtained from NASA was generated from daily satellite measurements of Level-2 quality. During Level-3 processing NASA maps the daily $1\,\mathrm{km}$ resolution products to a $4\,\mathrm{km}$ grid and applies several quality control checks, which are stored as a separate product into a 32-bit mask. These quality checks are made for different defined conditions as tabulated for Level-3 processing in table 2.1. If certain conditions exist for a pixel a flag is raised and the pixel is masked as not valid. A pixel may become invalid due to algorithm failure or due to the presence of atmospheric or oceanic conditions that can not be corrected for, e.g. contamination due to severe sun glint or stray light. All flagged pixels are then excluded from further analysis. NASA delivered Level-3 standard mapped products in the Hierarchical Data Format (HDF), which contain objects in two-dimensional arrays on an Equidistant Cylindrical (also know as Platte-Carrée) projection of the globe.

In a first processing step (figure 1.2) CSIRO reduced the global data set to monthly data covering only the North Marine Region $(127°\mathrm{E}-143°\mathrm{E}$ and $8°\mathrm{S}-18°\mathrm{S})$. In a second step the reduced data was aggregated into each six wet and dry seasons covering 2002 to 2008. The wet season was defined as period between April and October each year, while the dry season encompasses the period between November and March each year.

Table 2.1: Quality control flags for the remote sensing products in this study with associated product bit number.

Condition indicated / Flag	Bit
Atmospheric correction failure	1
Pixel is over land	2
Severe sun glint	4
Observed radiance very high or saturated	5
High sensor viewing angle	6
Stray light contamination	9
Clouds and/or ice contamination	10
Coccolithofores detected	11
High solar zenith angle	13
Low water-leaving radiance (cloud shadow)	15
Derived product algorithm failure	16
Questionable navigation (e.g. tilt change)	17
Aerosol iterations exceeded maximum	20
Derived product quality is reduced	22
Atmospheric correction is suspect	23
Navigation failure	26

2.5 Bathymetry data

To compute the percentage light availability at sea bed based on equation 2.1 a bathymetry data set compiled by Geoscience Australia from seismic and sampling surveys as well as satellite altimetry estimates, was used (*Webster and Petkovic*, 2005). This data set covers an area of 41 million square kilometers of the Australian marine jurisdiction lying between $92°\mathrm{E} - 172°\mathrm{E}$ and $8°\mathrm{S} - 60°\mathrm{S}$. This high resolution data has a 9 arc second grid, which corresponds to approximately $250\ \mathrm{m}$ at the equator resulting in $32\,003 \times 20\,803$ grid cells. This data set was resampled to fit the North Marine Region, merged with light attenuation coefficients and sub-sampled to the Equidistant Cylindrical satellite data grid by averaging all bathymetry cells that have centres within a satellite grid cell. Figure 2.2 shows the resulting sub-sampled bathymetry covering the project area of the North Marine Region.

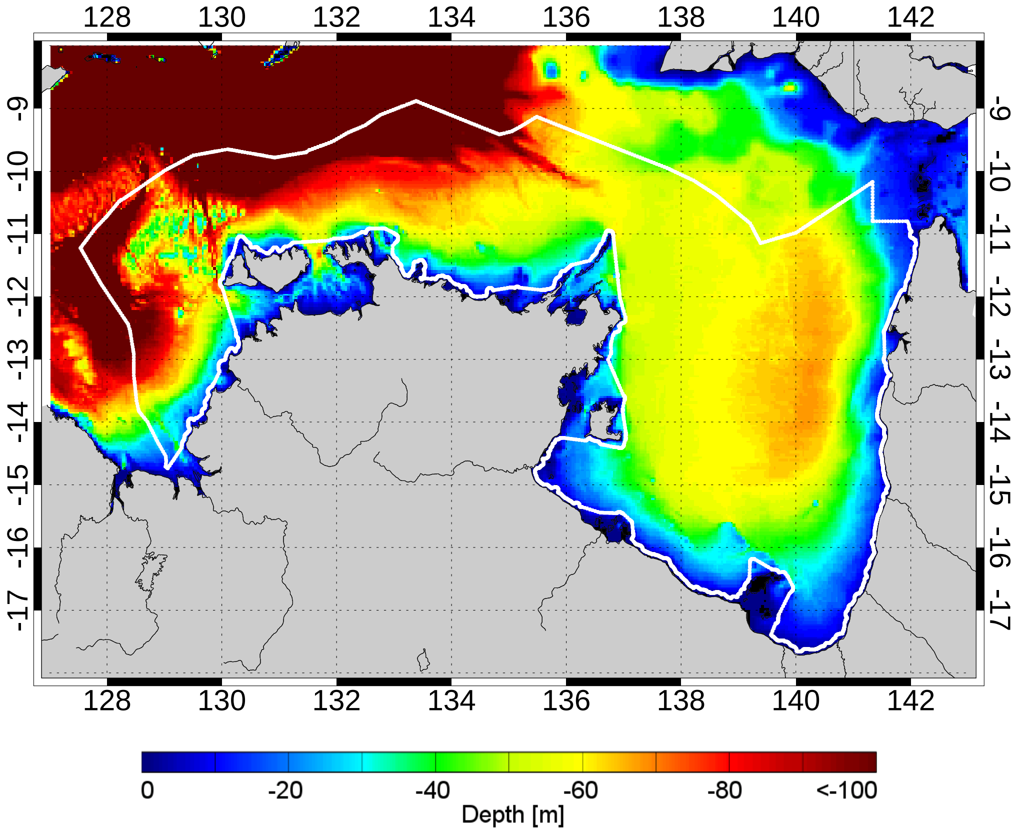

Figure 2.2: Sub-sampled bathymetry data with boundary of the North Marine Region.

Chapter 3

The environment of the North Marine Region

This chapter provides a brief introduction into the environment of the North Marine Region to assist in data interpretation.

From an aquatic remote sensing perspective this region is poorly investigated and understood because of the optical complexity of its water masses. Seasonal floods caused by monsoonal rainfall provide high loads of sediments and nutrients to the coastal zone. Tropical cyclones and strong tidal currents have a pronounced effect on the mixing of the water constituents including resuspension of sediments. The off-shore waters of the North Marine Region are nevertheless optically complex with large algal blooms (Coccolithophore and Trichodesmium species) occurring during the dry season months, in particular in the Gulf of Carpentaria. This large variability in optical properties and their non-linear contribution to the remote sensing signal causes large errors from global ocean colour algorithms. Global algorithms work accurately for open ocean waters where the optical properties are determined solely by phytoplankton, degradation products and the water itself. In coastal waters the presence of dissolved organic and particulate inorganic material from run-off or resuspension lead to inaccurate chlorophyll estimates from global algorithms (*Qin et al.*, 2007). Region-specific ocean colour algorithms currently do not exist for the North Marine Region but improved algorithms may be implemented based on parameterisations derived from in-situ measurements. Such regional parameterisations have been successfully implemented before by CSIRO in other optically complex Australian coastal waters (*Schroeder et al.* 2008; *Brando et al.* 2008).

Other, more common remote sensing applications in the North Marine Region include radar applications to estimate sea surface height and infrared applications to estimate sea surface temperature.

The following brief summary of the most relevant processes and drivers with regard to this project are citations taken from more comprehensive summaries published by *DEWHA* (2007) and *DEWHA* (2008).

- »The North Marine Region is characterized by a tropical monsoon climate. Wind strength, wind direction and rainfall vary dramatically between the wet and dry season, resulting in seasonal differences in water column mixing, turbidity, productivity, salinity, waves and wind-driven surface currents.«

- »From October to March monsoon winds are mostly northerly or north-westerly and vary in intensity. From April to September south-easterly trade winds predominate, being both stronger and more consistent than the monsoonal winds.«

- »Strong dry season trade winds result in well-mixed waters in the central Gulf (of Carpentaria). During the wet season, the monsoon winds tend to be weaker and less consistent, so that the central Gulf waters become stratified because of higher surface water temperatures, creating a well-mixed layer of surface waters and a cooler bottom layer of well-mixed waters. In contrast, coastal Gulf waters remain well mixed throughout the year.«

- »Cyclones create large disturbances across shallower parts of the Region, with impacts ranging from localised damage to coral reefs, to widespread turbidity and the mobilisation of sediments.«

- »While there are no major ocean currents in the North Marine Region, tidal currents are a significant force in the movement of water and biota, and mobilisation of bed sediments throughout the Region. Currents are particularly strong inshore around islands and reefs, and offshore in channels, canyons and valleys that drain off the shelf. Tidal currents are primarily responsible for the localised upwellings that occur around reefs, banks and islands.«

- »The large rivers of Papua New Guinea and Indonesia also deliver enormous quantities of sediment, freshwater and nutrients into the oceans to the north of the Region. These inputs are likely to affect the productivity of the offshore waters of the North Marine Region, although the extent of their influence is unknown. Productivity in offshore waters is predominantly associated with upwellings, eddies and currents, which bring nutrient-rich bottom water into the photic zone. Nutrients may be re-suspended in the water column through disturbance by winds, tides, waves, currents and cyclones.«

- »Monsoonal rainfall generates enormous quantities of freshwater, sediment and nutrients that enter coastal waters during the wet season. These terrestrial inputs are trapped within the coastal boundary layer, a body of turbid, eutrophic and highly productive inshore water that follows the coastline of the North Marine Region, extending out to a depth of approximately 30 m. The detritus and nutrients derived from mangroves, salt marshes and mudflats are fundamental to the functioning of coastal marine ecosystems in the Region. Very little mixing occurs between turbid coastal boundary layer waters and clear (oligotrophic) offshore waters, and hence there is little transfer of nutrients, freshwater or sediments into offshore waters. The junction of the two water bodies can be observed as a visibly distinct line during both the wet and dry season. During the dry season, there is little connection between river waters and the coastal sea, and the »inverse estuaries« of northern Australia actually pump water and sediments landward.«

- »The interplay between predominantly dry south-east trade winds from May to October and moister north-westerlies over the wet season (December to March) contributes to the slow, clockwise movement of water in the Gulf of Carpentaria.«
- »Ninety seven per cent of the area of the North Marine Region lies over the continental shelf at depths of less than 200 m. Across most of the Region, including the Gulf of Carpentaria which is the largest tropical epicontinental sea in the world, the water depth does not exceed 70 m. Maximum depths occur at around 350 m in the canyons of the Timor Transition.«

Chapter 4

Results and discussion

This chapter presents the inter-annual variations of light attenuation based on monthly averages (Appendix B). Further, we discuss the results of wet and dry season light attenuation aggregation and its subsequent merging with bathymetry data to calculate the percentage light availability at sea bed.

4.1 Monthly data

Appendix B provides an inter-annual overview of all monthly averaged light attenuation maps used within this project. The data set covers in total 72 months of the period between November 2002 and October 2008. Black colour-coded pixels are associated with clouds, bad quality or algorithm failure and are masked according to the quality control flags as referenced in table 2.1. Often, some of the near-shore regions reveal masked values throughout the year, most likely caused by atmospheric correction failure over turbid waters. These masked near-shore regions often lie within three nautical of the coast; a zone under the responsibility of the Queensland and Northern Territory Governments. In addition we find larger areas of masked values during the wet season months (November to March) due to frequent cloud cover resulting in a low number of valid pixels, especially during January and March 2006. The inter-annual monthly data set reveals that the light attenuation in the North Marine Region undergoes a seasonal cycle showing some distinct regional patterns.

- During the wet season the highest turbidity values are observed for near-shore coastal areas due to the sediment and nutrient rich run-off after monsoonal rainfall. In particular, March 2008 is a good example that shows the extent to which turbid waters may reach into the Gulf of Carpentaria during the end of the wet season. The data also confirms previous findings as summarized by *DEWHA* (2007) that the run-off is largely trapped within the coastal boundary with only limited exchange between coastal and off-shore waters. The off-shore waters show much lower turbidity and little variability during the wet season months, except for March 2003 when a large-scale pattern (presumably an algal bloom) appears in the Gulf of Carpentaria.

- With the beginning of the dry season in April, we observe an increase in turbidity and in its variability caused by a growth in productivity, which can be seen throughout the North Marine Region. This general increase of turbidity is consistent with previous findings compiled by *DEWHA* (2007) of well-mixed water conditions caused by prevailing strong dry season trade winds, especially in the Gulf of Carpentaria. In addition, frequently immense algal blooms occur in the Gulf of Carpentaria and the Joseph Bonaparte Gulf enhancing the dry season turbidity levels, especially during the month of June.

4.2 Aggregated dry and wet season data

Figure 4.1 shows the final result of the light attenuation aggregation into dry and wet season averages based on the monthly averages of the North Marine Region (Appendix B). To examine the regional differences between the aggregated dry and wet seasons we calculated the percentage difference between the seasons compared to the annual mean attenuation $\overline{K_\mathrm{d}} = \left(\frac{K_\mathrm{d}(\mathrm{wet})+K_\mathrm{d}(\mathrm{dry})}{2}\right)$ as shown in figure 4.2. The following features can be noted from figure 4.1 and 4.2:

- The aggregated dry and wet season averages exhibit no data of aggregated gaps from prior masked pixels as present in the monthly data set due to the much longer averaging period of each six dry and wet seasons.

- The aggregated data captures well the seasonal cycle and the regional differences of the monthly data. In detail, both seasons show the expected pattern of higher light attenuation in coastal waters due to higher concentration of organic and inorganic particles and coastal boundary trapping compared to lower attenuation values for the off-shore regions associated with less turbid waters.

- Near coastal turbidity is at a maximum during wet season, while off-shore turbidity peaks during the dry season. This pattern is illustrated in figure 4.2 by the percentage differences in K_d between aggregated dry and wet seasons compared to the annual mean ($\overline{K_\mathrm{d}}$). Areas in red colour (wet > dry) show this percentage increasing during wet seasons, while blue areas indicate percentage increase during dry seasons (dry > wet).

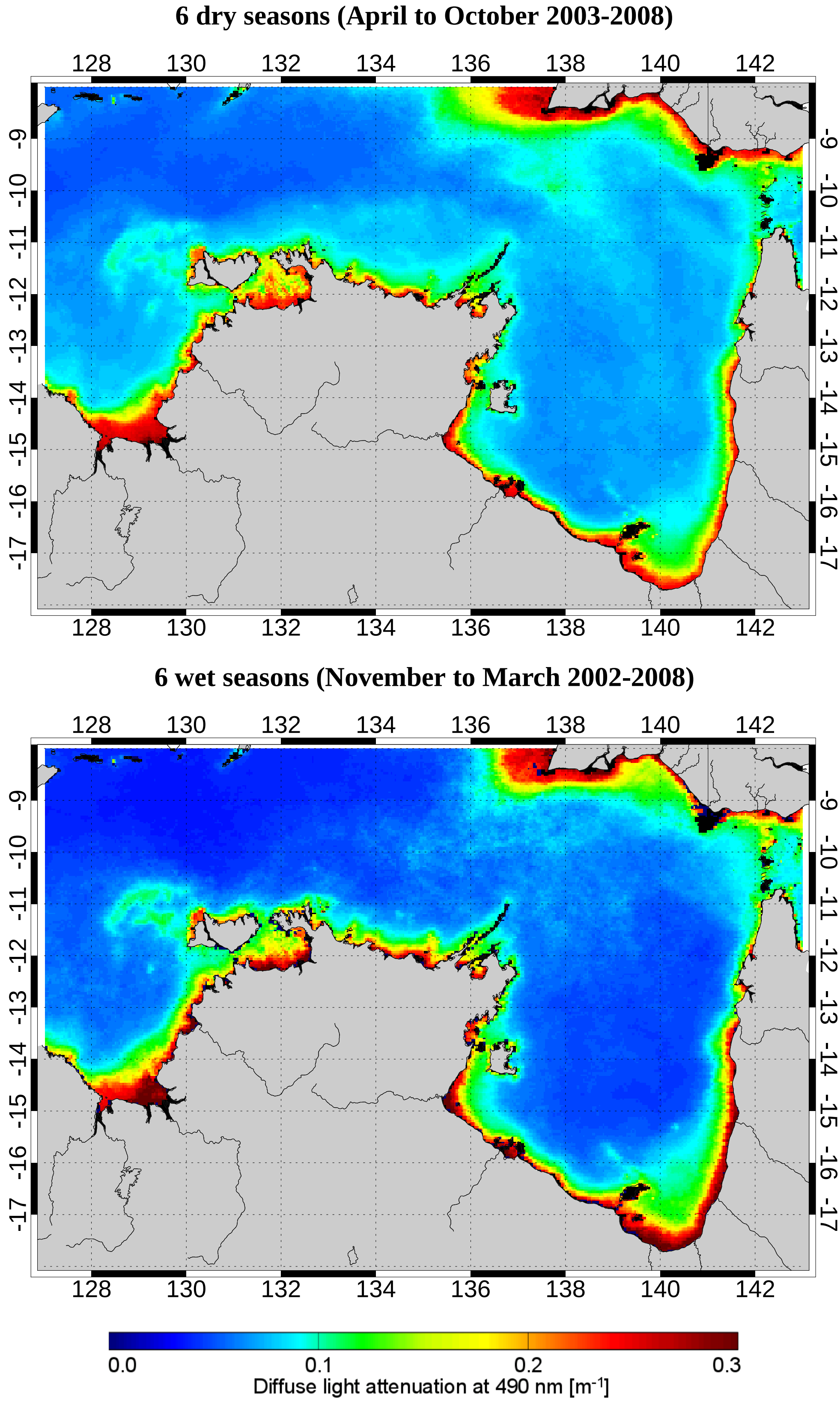

Figure 4.1: Aggregated dry and wet season averages of the diffuse light attenuation coefficient at 490 nm.

- With reference to the annual mean, we observe a wet season coastal turbidity increase of up to 50% compared to the dry season (red areas figure 4.2 with wet>dry), which can be explained by run-off after monsoonal rainfall.
- Further, we observe dry season off-shore turbidity increase of up to 50% compared to the wet season (blue areas figure 4.2 with dry>wet), which is explained by the occurrence of algal blooms and well-mixed conditions induced by prevailing strong trade winds.
- In contrast to the assumption that the large rivers of Papua New Guinea and Indonesia are unlikely to effect the productivity of the offshore waters of the North Marine Region (*DEWHA*, 2007), we observe a band of slight turbidity increase [$134°\mathrm{E} - 138°\mathrm{E}$ and $9°\mathrm{S} - 10°\mathrm{S}$, figure 4.2] influencing the Arafura Sea during the wet season. This influence can also be observed in some of the monthly maps. Further analysis on daily data is recommended to better understand the maximum extent of this influence.

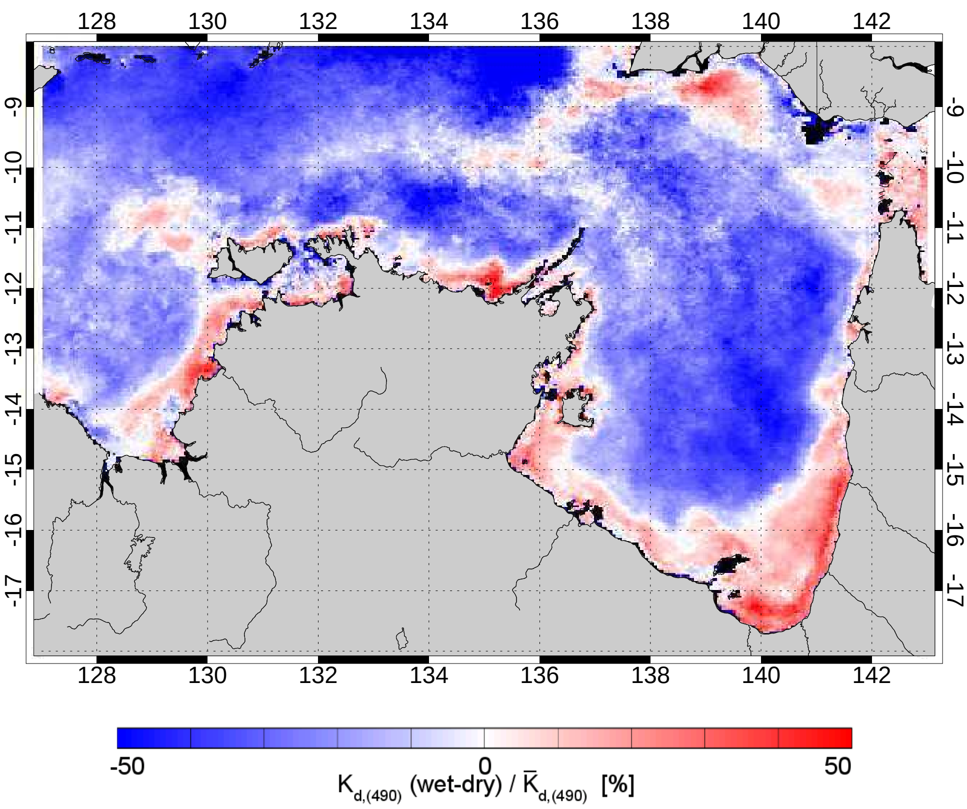

Figure 4.2: Relative difference between the aggregated dry and wet season light attenuation at 490 nm with reference to the annual mean attenuation ($\overline{K_\mathrm{d}}$).

Finally the percentage light availability at sea bed is calculated by merging the bathymetry data with the aggregated dry and wet season averages (equation 2.1). This light availability data offers the possibility to be used as a surrogate to predict benthic biodiversity. The concept of the euphotic depth may be applied by DEWHA for further analysis in the marine bioregional planning process. Aquatic biology defines the layer of the water that is exposed to sufficient sunlight for photosynthesis to occur as the euphotic layer. Significant phytoplankton photosynthesis takes place only down to a depth at which the downwelling irradiance (equation 2.1) of the photosynthetic available radiation falls to 1% of that just below the surface. The layer in which the irradiance falls to 1% marks the euphotic zone (*Kirk*, 1994) and is the only region in the water column where primary production occurs. The euphotic depth depends on the turbidity of the water and typical values range from a few centimeters in extremely turbid coastal or inland waters to approximately $200\,\mathrm{m}$ in the open ocean.

It must be noted that while the above definition of the euphotic zone considers a light threshold based on photosynthetic available radiation (PAR), which is an integral measure of the light between 400 and 700 nm, the percentage light availability for this project is based on estimations at a wavelength of 490 nm only. Figure 4.3 shows four different threshold maps (1, 5, 10, 20%) of light availability at the sea bed for each dry and wet season aggregation. Pixels below the designated threshold are mapped in black, whereas valid pixels are colour-coded in green. However, the digital data does not contain any predefined thresholds, given that threshold levels may be variable and need to be determined for specific applications. The following features can be noted from the light availability at sea bed in figure 4.3:

- The area of the sea bed that receives 1% of the surface light covers nearly the entire North Marine Region during both dry and wet seasons, except for the deeper ocean areas of the Arafura Sea and Joseph Bonaparte Gulf with depths greater than 80-100 m. Parts of the Gulf of Carpentaria receives on average less that 1% light during the dry seasons, while entire Gulf receives a minimum of 1% during the wet seasons.

- Setting a minimum threshold of 5% reduces the areas both in dry and wet season dramatically. The central part of the Gulf of Carpentaria deeper than 40 m now receives less than 5% of the surface light during dry seasons. During wet seasons these areas increase for the central part of the Gulf of Carpentaria as a result of lower turbidity.

- A further reduction of the light threshold to a minimum of 10% confines mapped areas to a near-shore boundary showing no major differences between dry and wet seasons.

- A minimum of 20% of the surface light is only received by the near-shore areas and parts of the Torres Strait with no major differences between dry and wet seasons.

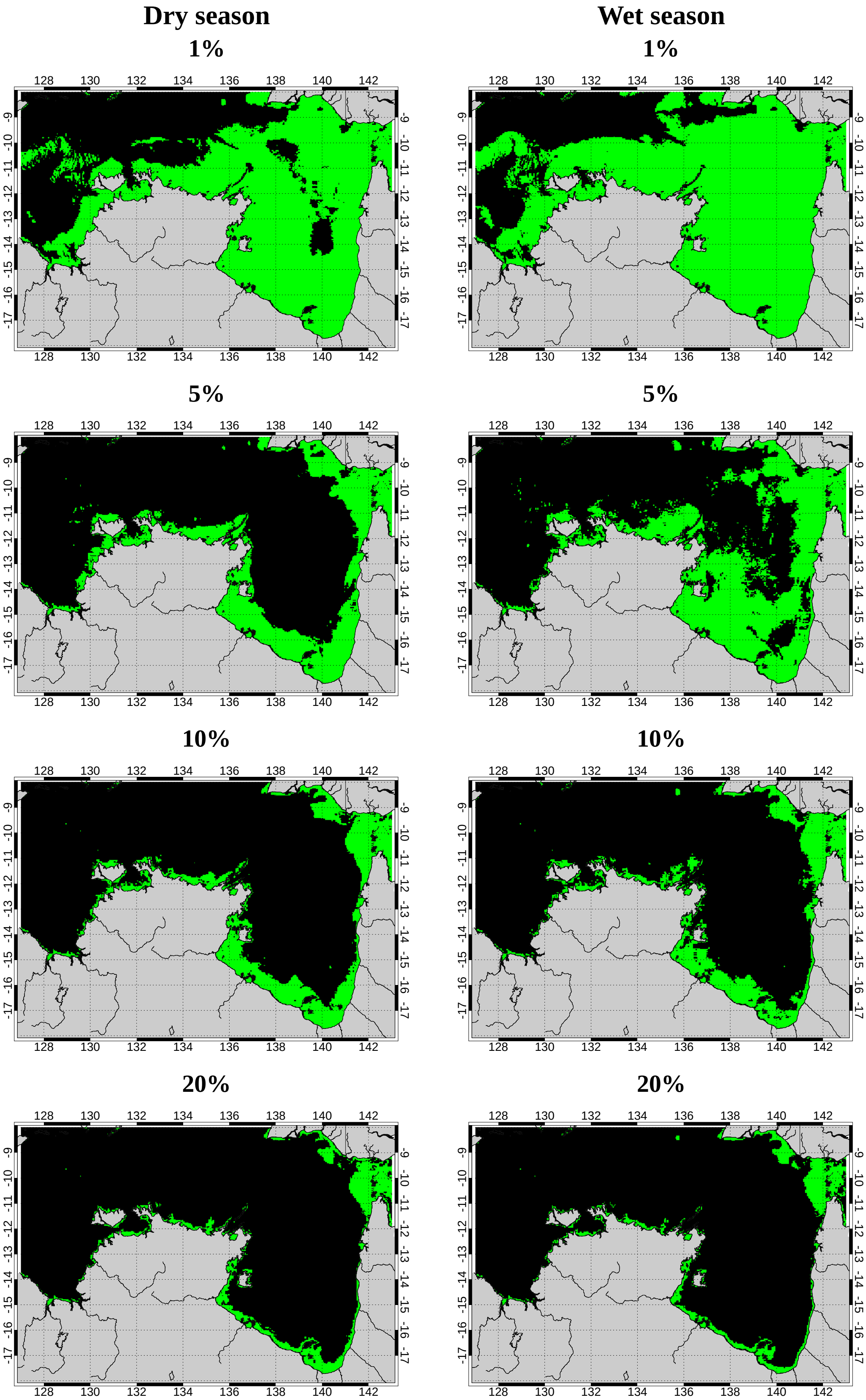

Figure 4.3: Percentage light availability at the sea bed for aggregated dry and wet seasons and four different thresholds. Pixels below the designated threshold are colour-coded in black.

Chapter 5

Conclusion and future directions

The key conclusions from this data analysis are:

1. The inter-annual monthly data set reveals that the light attenuation in the North Marine Region undergoes a distinct seasonal cycle.

2. During the wet seasons (2002 to 2008) highest turbidity values are observed for the near-shore coastal areas due to sediment and nutrient rich run-off after monsoonal rainfall. The off-shore waters in contrast show much lower turbidity and little spatial variability.

3. During the dry seasons (2002 to 2008) a general increase of turbidity combined with larger spatial variability is observed for all off-shore regions of North Marine Region due to trade winds-induced mixing and algal blooms occurrence. The coastal regions show a decrease in turbidity from reduced run-off.

4. During both dry and wet seasons the region of highest turbidity is observed along the coastline trapped within the coastal boundary with depths less than 20 meters.

5. The aggregated dry and wet season data captures well the seasonal cycle and the regional differences of the monthly data.

6. With reference to the annual mean attenuation, the near-shore regions show up to 50% higher turbidity values during the wet seasons compared to the dry seasons (2002 to 2008), while the off-shore regions show up to 50% higher turbidity values during the dry seasons compared to the wet seasons (2002 to 2008).

7. During wet seasons the large rivers of Papua New Guinea and Indonesia slight increase turbidity levels within the northern part of the North Marine Region (Arafura Sea).

8. Percentage light availability at the sea bed was calculated by merging bathymetry with light attenuation. The resulting digital data set does not contain any pre-defined thresholds; these need to be established by DEWHA under consideration of the different scenarios within the marine bioregional planning process.

Recommendations for future applications within the North Marine Region are:

1. Currently available global algorithms can only provide limited product accuracy for the North Marine Region; CSIRO recommends to implement regional algorithms, which require prior in-situ measurements for parameterisation. These algorithms would provide more accurate estimates of chlorophyll-a, suspended matter and coloured dissolved organic matter, from which primary productivity estimates may be calculated. Further, these algorithms would give more accurate estimates of light attenuation in coastal waters (refer to section 2.3) and provide error maps for quality control.

2. In addition, sea surface temperature combined with chlorophyll data and sea surface currents from satellite altimeter may be used to detect highly productive upwelling water mass areas in the North Marine Region.

Acknowledgements

We are grateful to the CSIRO National Research Flagship Wealth from Ocean and the Department of the Environment, Water, Heritage and the Arts for funding this project. Further we acknowledge the MODIS mission scientists and associated NASA personnel for the production of the data used in this research effort.

Bibliography

Austin, R. W., and T. J. Petzold, *Oceanography from Space*, Chapter: The determination of the diffuse attenuation coefficient of sea water using the coastal zone color scanner, Pages 239–256, Springer, New York, 1981.

Brando, V. E., A. G. Dekker, T. Schroeder, Y. J. Park, L. Clementson, A. Steven, and D. Blondeau-Patissier, Satellite retrieval of chlorophyll CDOM and NAP in optically complex waters using a semi-analytical inversion based on specific inherent optical properties. A case study for Great Barrier Reef coastal waters, in *Proceedings of The XIX Ocean Optics Conference, Barga, Italy*, 2008.

Church, J. A., and A. M. G. Forbes, Circulation of the Gulf of Carpentaria. I Direct Observations of Currents in the South-east Corner of the Gulf of Carpentaria, *Aust. J. Mar. Freshw. Res.*, *34*, 1–10, 1983.

DEWHA, Characterization of the Marine Environment of the North Marine Region, *Report: Outcomes of an expert workshop*, DEWHA, 2007.

DEWHA, The North Marine Bioregional Plan - Bioregional Profile, *Report: A description of the ecosystems, conservation values and uses of the North Marine Region*, DEWHA, 2008.

J. E. O'Reilly and 24 Co-authors , SeaWiFS Postlaunch Calibration and Validation Analyses, Part 3, *NASA Tech. Memo. 2000-206892*, *11*, 49, 2000.

Kirk, J. T. O., *Light and Photosynthesis in Aquatic Ecosystems*, Cambridge University Press, 1994.

Lee, Z. P., M. Darecki, K. L. Carder, C. O. Davis, D. Stramski, and W. J. Rhea, Diffuse attenuation coeffcient of downwelling irradiance: An evaluation of remote sensing methods, *Journal of Geophysical Research*, *110*, C02,017, doi:10.1029/2004JC002,573, 2005.

Pope, R. M., and E. S. Fry, Absorption spectrum (380-700 nm) of pure water. II. Integrating cavity measurements, *Appl. Opt.*, *36*, 8710–8723, 1997.

Qin, Y., V. Brando, A. Dekker, and D. Blondeau-Patissier, Validity of SeaDAS water constituents retrieval algorithms in Australian tropical coastal waters, *Geophysical Research Letters*, *34*, L21,603, doi:10.1029/2007GL030,599, 2007.

Schroeder, T., V. E. Brando, N. Cherukuru, L. Clementson, D. Blondeau-Patissier, A. G. Dekker, and J. Fischer, Remote sensing of apparent and inherent optical properties of Tasmanian coastal waters: Application to MODIS data, in *Proceedings of The XIX Ocean Optics Conference, Barga, Italy*, 2008.

Webster, M. A., and P. Petkovic, Australian Bathymetry and Topography Grid, June 2005, *Record 2005/12*, Geoscience Australia, 2005.

Xiong, X., and W. Barnes, An Overview of MODIS Radiometric Calibration and Characterization , *Advances in Atmospheric Sciences*, *23*, 69–79, 2006.

Appendix A

Glossary of Terms

Attenuation: The reduction with distance from the source of the intensity of an acoustic or an electromagnetic signal propagating through a medium caused by scattering and absorption processes.

Irradiance: A radiometric term for the rate at which radiant energy in a radiation field is transferred across a unit area of a surface (real or imaginary) in a hemisphere of directions.

Nadir: Satellite subpoint on the earth's surface that is centered directly below the satellite.

Radiance: A radiometric term for the rate at which radiant energy in a set of directions confined to a unit solid angle around a particular direction is transferred across unit area of a surface (real or imaginary) projected onto this direction.

Wavelength: In radiation, the distance between periodic spatial repetitions of an electromagnetic wave at a given instant of time; used extensively to classify the nature of the radiation, since most of the interactions between radiation and matter are extremely sensitive to the wavelength of the radiation.

Appendix B

Inter-annual monthly mean light attenuation maps

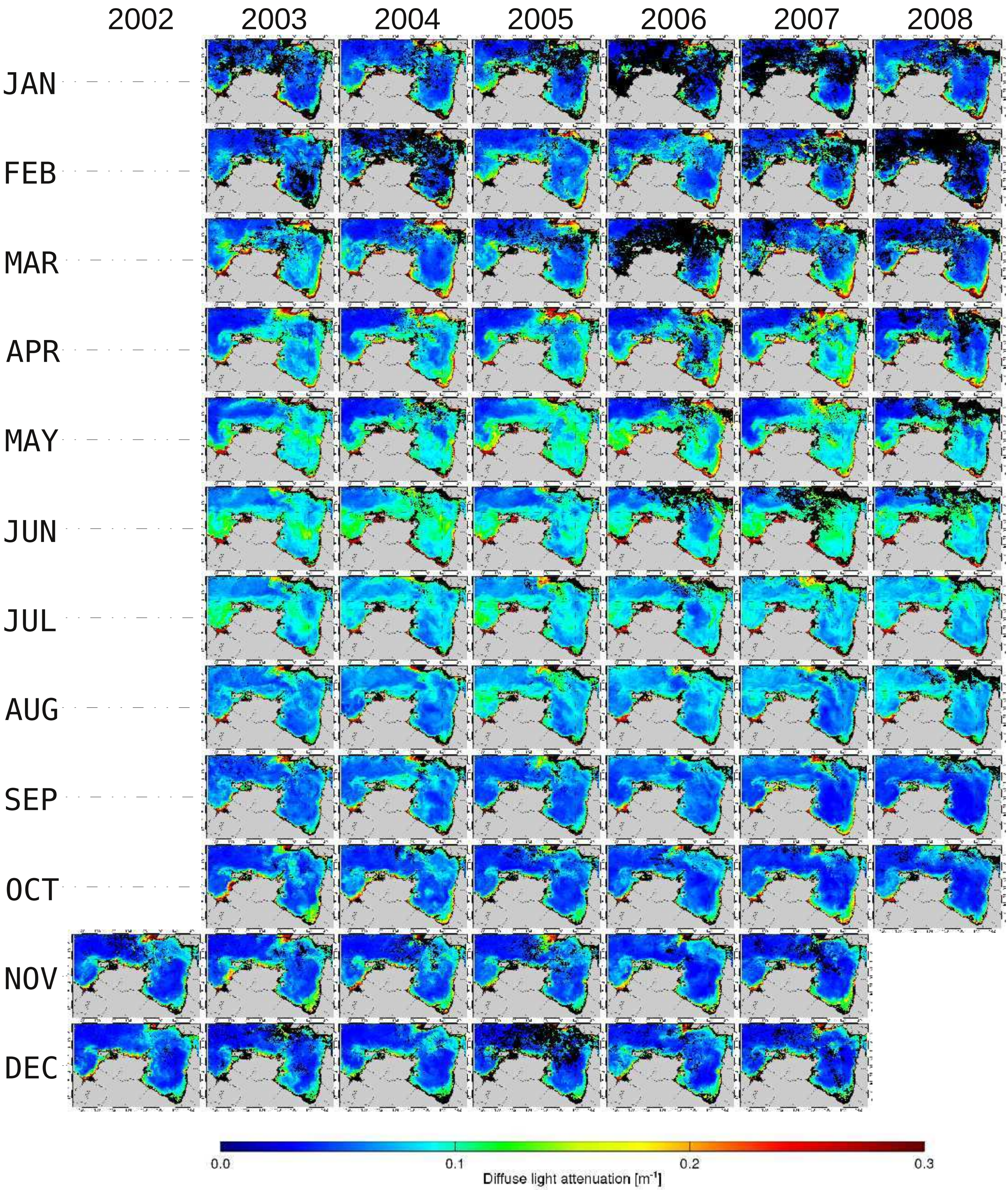
2002
2003
2004
2005
2006
2007
2008
JAN
FEB
MAR
APR
MAY
JUN
JUL
AUG
SEP
OCT
NOV
DEC
0.0
0.1
0.2
0.3
Diffuse light attenuation [m-1]

Contact Us
Phone: 1300 363 400
+61 3 9545 2176
Email: enquiries@csiro.au
Web: www.csiro.au

Your CSIRO

Australia is founding its future on science and innovation. Its national science agency, CSIRO, is a powerhouse of ideas, technologies and skills for building prosperity, growth, health and sustainability. It serves governments, industries, business and communities across the nation.